Mineralogical evolution of salt over nine years, after removal of efflorescence and saline crusts from Elche's Old Bridge (Spain)

Salvador Ordóñez[a, b, *]

salvador@ua.es

Ángel La Iglesia[b, c]

iglesia@geo.ucm.es

Miguel Louis[b, d]

miguel.louis@ua.es

Mª Ángeles García-del-Cura[b, c]

agcura@geo.ucm.es

[a]Departamento de Ciencias de la Tierra y del Medio Ambiente, Universidad de Alicante, San Vicente del Raspeig, 03690, Spain

[b]Laboratorio de Petrología Aplicada, Unidad Asociada Universidad de Alicante-CSIC, San Vicente del Raspeig, 03690 Alicante, Spain

[c]Instituto de Geociencias (IGEO, CSIC, UCM), Facultad de Geología, c/ José Antonio Novais, 12, 28040 Madrid, Spain

[d]Departamento de Construcciones Arquitectónicas, Universidad de Alicante, San Vicente del Raspeig, 03690, Spain

*Corresponding author at: Departamento de Ciencias de la Tierra y del Medio Ambiente, Universidad de Alicante, San Vicente del Raspeig, 03690, Spain.

Abstract

The Old Bridge Elche's showed abundant efflorescence and salt crusts that were eliminated in an intervention in 2005. We have followed the development of efflorescence after the intervention. And nine years later the efflorescence mineralogy was quite similar to the mineralogy of the pre-restoration efflorescence.

The efflorescence on Elche's Old Bridge (*Puente Viejo*) shows a wide mineralogical variation in the vertical profile, which is the result of a balance between two diffusive processes: the evaporation–condensation of atmospheric water vapor on/inside the wall, and the capillary flow of saline groundwater. Diurnal variations in atmospheric relative humidity (RH) and the low deliquescence relative humidity (DRH) values of some saline minerals (nitrate & chloride) play an important role in the vertical distribution of minerals.

The mineral composition of efflorescence and saline crusts prior to cleaning the monument was similar to that identified nine years later.

The chemical composition of groundwater, with a high sodium chloride component and much lower concentrations of sulfate and bicarbonate, explained the presence of halite, while the presence of demolition waste of a gypsiferous nature near the bridge explained the presence of sulfate salts, thenardite, konyaite, aphthitalite, and arcanite. The dissolution of airborne particles in condensation water probably contributed to the genesis of nitrate-rich minerals such as nitratine, darapskite, and especially humberstonite.

Keywords: Efflorescences; Salt damage stones; Capillary water; Condensation water; MDRH (mutual deliquescence relative humidity); DRH; RH; Single salts; Double salts; Humberstonite

1 Introduction

1.1 Elche's Old Bridge

The bridge under study is located in Elche, an industrial city in the province of Alicante (Region of Valencia, SE Spain; 38°16′01″ N, 0°41′54″ W and 86 m above sea level). A small river or stream called the Vinalopó flows though Elche, dividing it in half, and the Old Bridge (*Puente Viejo*, also known as the *Puente Santa Teresa*) is one of the ten bridges that unite both parts of the city.

The Old Bridge was built between 1750 and 1756. Work began on the construction of a stone bridge in 1705, but a flood in 1750 destroyed the early works and the bridge was subsequently redesigned with a double arch and a cutwater in the late Gothic style (Fig. 1). The bridge consists of two ashlar arches with a central pilaster including a cutwater. The arches are supported by the central pillar and on the river banks, out of the water. The external surfaces of the arches, the pillar and cutwater are made of ashlar masonry, using concerted masonry, while the lateral parts of the bridge are made of rubble masonry. The inner part of the bridge is filled with compressed soil, which had been removed during restoration to reveal the arches' inner faces [1]. In previous interventions, hygroconvectors had been placed at some points to eliminate possible humidity in the stonemasonry.

Fig. 1 General view of Elche' Old Bridge, facade N, after restoration (2006).

Two small stone buildings (chapels) sit in the center of the bridge at the top. These were cleaned in the 1970 s and their stones were replaced by Bateig stone, a material with similar petrophysical properties [2] to those of the original material.

By 2004, the Old Bridge was showing significant surface damage on the abutments, the vault, and the south side, and restoration was carried out in 2005. During this process [1], the ashlar was cleaned and repaired and a preventive treatment was applied; the efflorescence was removed by means of microabrasion using aluminum silicate powder, and then FK-12 (salt and microorganism remover from Fakolith Co.), Tecosel cleaner and salt inhibitor (Edylteco Co.) and a water repellent were applied. Falconit Elite repairing mortar was applied to specific areas in order to repair small breaks. Where the ashlar had merely suffered a fissure, these narrow openings were filled by means of epoxy F/G mortar injection, made from low viscosity, high penetration thixotropic epoxy resins. The outer surface was sealed using the same mortar as that used in the repointing process. Spandrel fill material was removed during the 2005 restoration and replaced by a filler of the same type. The most severely damaged masonry was the ashlar blocks comprising the bridge abutments, and some of these were replaced in 2005 by recycled San Julian Stone [1]. San Julian Stone is a variable-sized sandy biocalcarenite with variable fossil typology (bryozoans, mollusks, foraminifera and red algae) that is quarried in Alicante and has been used in numerous constructions in this town. The properties of this stone vary according to its stratigraphic position.

In spite of the restoration carried out in 2005, by 2008 the bridge abutment and arch barrel surface again presented salt efflorescence on building stones and joint mortar and related damage. The main focus of the present paper is a study of the salt deposits formed on the south side of the bridge (asterisk in Fig. 2A).

Fig. 2 South side of the bridge. A. Cleaning and sampling of salt vault efflorescence (arrow) (2005). Asterisk shows the preferred study area in this paper. B. View of sampled abutment of the bridge at 2008.

1.2 Climatic environment

Elche has a semiarid climate with an average annual/ monthly temperature of 17.2 °C, a maximum average temperature of 29 °C, and a minimum monthly average temperature of 0.19 °C for January, according to data recorded for the period 1999–2014 at the Elx station of the Agro-climatic Information System for Irrigation http://eportal.magrama.gob.es/websiar/.

In the period 2005–2013, only 7 cloudy days and 84 rainy days per year were recorded at the nearby airport of El Altet, totaling an average of 250 mm/year of rainfall, while the maximum temperature recorded was 38.6 °C in August 2010. There is a prevailing south wind, with annual average wind direction values of 182° ± 62° (approximately 64% of probable values are in this range). This aspect, together with the sunshine, may explain why there is more evaporation on the south side than on the north wall of the Old Bridge.

Relative humidity (RH) shows dramatic diurnal and monthly variations. The prevailing wind direction in this region is northwesterly in winter and from the sea during the summer. Solar radiation is quite intense, with a daily average above 250 W m^{-2} during the greatest part of the spring and summer, and shows a Saharan dust influence, with inorganic ions $SO_4^{=2}$, NO_3^{-1}, NH_4^{1+} in the summer months [3]. The atmospheric aerosols of Elche studied from December 2004 to November 2005 were very complex [3], with the major components of the fine fraction PM2.5 (suspended particulate matter with a diameter of 2.5 μm or less), accounting for 40% of the total mass. In the coarse fraction PM10 (suspended particulate matter with a diameter of 10 μm or less), nitrate (as $NaNO_3$ and $Ca(NO_3)_2$), together with crustal ($CaCO_3$) and marine species (NaCl) accounted for almost 50% of the total mass.

1.3 Objectives

The main objectives of this paper are;

a) To describe the evolution over nine years of the mineralogy and textures of salt deposits formed on a monument restored in 2005. Nine years was the time when the efflorescence developed after the intervention reached the composition pre-intervention.

b) To compare post-restoration salts in efflorescence and saline crusts with pre-intervention salts.

c) To analyze the role of capillary water, infiltration water and moisture condensation waters in the genesis of efflorescence.

d) To propose a model to explain the origin of saline solutions leading to efflorescence, considering the chemical composition of capillary and seepage water, and also the nature of airborne particles.

e) The final objective of the paper, would provide information about the evolution of the mineralogy of efflorescence for future removal of salt crusts projects.

2 Materials and methods

2.1 Materials

Elche's Old Bridge is mainly built of biocalcarenites. Biocalcarenite quarries have been in use in this area since before Roman times, and yield what is known as Ferriol stone. Employed for sculpture by the Iberians [4], one petrologic type was used to sculpt the "Dama" of Elche, an emblematic Hellenistic Iberian sculpture dated to the fourth of ~~fifth~~ 5th century B~~.~~C~~E~~ [5].

Some stones in the Elche bridge show the petrographic and aesthetic characteristics of some Ferriol stones; the stones of the lower part of the stratigraphic series of the area in which these quarries are located.

Various types of biocalcarenite stone have been used in the bridge, mainly fine-grained foraminifera biocalcarenite formed mostly of globigerinae with some fragments of bivalve shells, but also sandy biocalcarenite with lime clasts, quartz grains, echinoderm, mollusk and bryozoan fragments, and foraminifers. The effective porosity of these building stones in the Old Bridge varies from 4 to 12%. At the base of the bridge, some conglomerate ashlar blocks are present with differential decay after clast lithology [1].

The salt deposits and efflorescence developed on the bridge abutment exhibit a rare mineralogy (Table 2). Of particular note is the presence of double salts, not too mentioned in architectural heritage salt damage. Some detailed studies of these salts refer to research on Andean salt flats and deposition of aerosol and dust from ventilation air and evaporation of groundwater and seeping into potential geologic repository for nuclear waste.

Table 1 Statistical parameters for ion concentrations in PM2.5 and in PM10 samples, for the period December 2004 to November 2005. After Nicolas et al. [3].

	PM2.5 (μg m^{-3})					PM10 (μg m^{-3})				
	%>LD (detection limit)	Mean	SD (standard deviation)	Min.	Max.	%>LD	Mean	SD	Min.	Max.
PM		15.4	9	3.6	54.6		34.3	15.5	9.3	73.8
Cl^-	61	0.18	0.22	0.04	1.13	100	0.6	0.5	0.06	2.27
NO_3^-	100	1.37	2.21	0.1	15.5	100	3.76	2.99	0.34	21.67
$nmSO_4^{2-}$	100	3.79	2.92	0.37	15.82	100	4.36	3.09	0.58	16.61
Na^+	79	0.27	0.11	0.13	0.54	100	0.99	0.72	0.13	3.32
Ca^{2+}	16	0.36	0.16	0.23	0.85	100	2.29	0.98	0.3	4.67
Mg^{2+}	92	0.02	0.01	0.01	0.11	100	0.16	0.1	0.02	0.46
K^+	68	0.21	0.16	0.07	1.27	100	0.28	0.26	0.07	2.09

Table 2 Minerals cited in the text and their chemical formulas.

Halite	NaCl
Thenardite	Na_2SO_4
Mirabilite	$Na_2SO_4{\cdot}10H_2O$
Konyaite	$Na_2Mg\ (SO_4)_2{\cdot}5H_2O$
Nitratine	$NaNO_3$
Humberstonite	$K_3Na_7Mg_2(SO_4)_6(NO_3)_2{\cdot}6H_2O$
Arcanite	K_2SO_4
Aphtitalite	$(K,Na)_3Na\ (SO_4)_2$

Sylvite	KCl
Darapskite	$Na_3(NO_3)(SO_4)\ H_2O$

2.2 Methods

The salts in crusts and efflorescence were sampled by scraping in 2005, 2008, 2011 and 2013 in the summer, after periods of more than one month without rain. The 2005 sampling was performed before restoration. In 2005, an elevator or articulated derrick installed for the restoration made it possible to take samples from the vaults (arrow in Fig. 2A) and facilitated sampling of the arches. In subsequent campaigns in 2008, 2011 and 2013, most sampling was performed on the south abutment of the bridge (Fig. 2B) which is where most of the efflorescence had formed.

Sampling of efflorescence and salt crusts was carried out on the base of the corridor that runs along the arch barrel and the belt course located 3.5 m above the spandrel masonry of the south wall of the bridge, left abutment. The maximum concentration of salts occurred at the point of vertical contact between the ashlar blocks forming the arch intrados, and the remains of ancient ashlar masonry, and also in the mortar joints of the spandrel. The lowest point of reference for the relative sampling height (RSH) of saline efflorescence and crusts was the corridor that runs along the abutment.

Saline soils of the left bridge abutment foundation have been sampled using a set of nozzles 1 cm in diameter, which could be obtained 20 cm thick cores, and were used to determine the soluble ions in the soil foundation.

The mineralogy of the salts found in the stones was determined by XRD and SEM with EDS. Chemical analysis of soils in the area was performed by XRF and ion chromatography.

2.2.1 XRD

The mineralogical composition of the powdered samples was studied by X-ray diffraction (XRD) using a Philips PW 1710 diffractometer with the following experimental conditions: Cu-Kα radiation, measurement interval of 2–65° 2θ, time per step 1 s, and a step size of 0.02 2θ. The mineralogical composition of the crystalline phases was estimated by XRD quantitative analysis, this was carried using the Bruker EVA software. With the same software, has achieved detection limits of 0.5%, in experimental mixtures of halite–thenardite, based on these results can be considered acceptable 1% values presented in this paper

2.2.2 SEM

Surface samples were observed with a Hitachi S 3000N variable pressure electron microscope (VPSEM) working at high pressure in secondary electron mode, using samples coated with a thin gold film produced with a SCD04 high vacuum evaporator. Uncoated surfaces were studied in low pressure backscattered electron mode using an EDS Bruker X Flash 3001 model in order to examine the compositional heterogeneity of the samples.

2.2.3 XRF

This technique was used to study the geochemical characteristics of the soil under the studied south abutment. All chemical analyses of the soil samples were performed by X-ray fluorescence (XRF) using an Axios Panalytical Spectrometer (Fig. 3).

Fig. 3 Efflorescence on the N face of the arch and on the vault. A. At 2008, B. North face of the arch at 2013. Outer surface is free from salts, but flaking and contour scaling are evident.

2.2.4 Ion chromatography

Determination of the chemical composition of the soluble salts in soils was performed by ion chromatography using a 761 Compact Metrohm IC with columns calibrated for F^{-1}, Cl^{-1}, NO^{2-}, NO^{3-}, SO_4^{2-}, and PO_4^{3-} anions and for Na^{+1}, K^{+1} and Ca^{2+} cations. Solutions consisted of 0.15 g of dried sample at 105 °C in 15 ml of ultrapure water (Millipore). For complete dispersion of the solid phase, the vials were maintained in an ultrasonic bath for 45 min and were subsequently centrifuged at 3500 rpm for 5 min.

3 Results

The principal damage observed, described after Fitzner & Heinrichs (2004) [6], was as follows:

Prior to restoration in 2005, some of the masonry presented broken fragments as well as signs of different forms of weathering: alveolar weathering, flaking, and differential decay in conglomerate materials [1]. Some ashlar blocks with vertical layering displayed the most intense alveolar weathering. Ashlar masonry in the bridge abutments had been the most severely affected, and some of the blocks were replaced in 2005. Graffiti had been drawn on these blocks, and their color had changed.

The inner faces of the vaults presented flaking (Figs. 2A, 3A and 3B), and the surface was altered by a strongly developed, light-colored efflorescence (arrow in Fig. 2A, essentially consisting of halite and thenardite (Fig. 4). The efflorescence was eliminated in the 2005 restoration process. But some years later, in 2008, we found them on the south side of the bridge, especially in the left abutment (Fig. 2B), which were probably accumulate from the end of 2005 restoration.

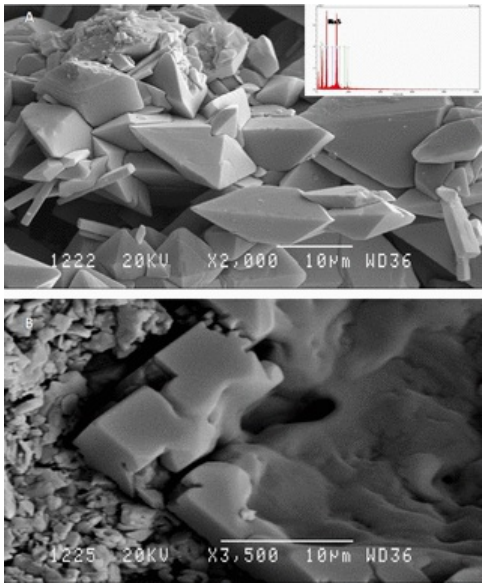

Fig. 4 SEM photomicrographs in se mode. A) Thenardite with EDS analysis. B) Halite with dissolution features.

3.1 Efflorescence and saline crusts: mineralogical composition

Before restoration was carried out on the south wall of the bridge, mainly on the abutment on the E side (asterisk in Fig. 2A and B), there was little flaking but efflorescence and saline crusts had formed with a complex saline mineralogy. XRD of the samples revealed the following crystalline phases: halite, thenardite, mirabilite, arcanite, darapskite, konyaite, humberstonite, nitratine, aphthitalite, and sylvite.

The saline efflorescence developed on the bridge abutment, have a complex mineralogy (Table 2). Of particular interest is the presence of double salts (sulfate-nitrate-Na-K-Mg), which have been little studied in the damage of architectural heritage, but have been cited in sculptures [7,8], bricks [9], plasters [10], and the overview of the salts influence on the damage to the architectural heritage have been described [11–13]. Detailed studies of the sequences of precipitation of these double salts in natural environments, can be observed in the Andean salt flats, as pointed out later.

3.2 The most relevant aspects of some of the most singular double salts found in efflorescence

Darapskite, which is widespread in the nitrate deposits of Chile, associated with halite, nitratine, and thenardite [14]. Its abundance is the result of the exceptionally high concentration of nitrate, and may be explained within the $NaNO_3$-NaCl-$NaSO_4$-H_2O system. According to Vega et al. (1996) [15], darapskite represents a mineral evolving from precipitation as the double sulfate salt, bloedite, to precipitation in the eutectic point of nitratine. However, it has also been identified by Oguchi et al. (2006) [16] in brick monuments. This mineral was identified in the efflorescence described here in significant amounts in the 2013 sampling.

K*onyaite*, which has been identified in efflorescence in saline environments [17,18], but which is also present on brick walls [16]. According to Buck et al. (2011) [19], it forms part of a group of minerals that respond quickly to changes in humidity and are hydrous / anhydrous.

Aphthitalite or glaserite, which is a non-hydrated potassium and sodium double sulfate, one of the rarer of the natural soluble sulfates, and has been reported in volcano efflorescence and in saline deposits [20]. It has been synthesized [21] from solid bittern treated with ClK in the 2ClNa-K_2SO_4-2ClK system. They have also been cited in decay processes in stone monuments [22] .

Humberstonite, which occurs in layers up to 40 cm thick in the nitrate fields in the Atacama desert, associated with bloedite and nitratine [23], and also in the region of Luobubo (China) [24]. In their review, Howley & Shettel (2004) [25] found that the genetic models of humberstonite are controversial, and it may be considered the result of leaching and recycling of old salt deposits in hydrothermal environments [26]. However, the most accepted theory is that the chemical composition of groundwater evolved with added marine aerosol and volcanogenic gas fallout, and that nitrate and chloride minerals are transported down the soil profile [27–29]. It is worth highlighting that humberstonite has rarely been detected in salt efflorescence on brick, masonry or ashlar walls [30].

3.3 Efflorescence and saline crusts: mineralogical composition

The mineralogical composition (%) and spatial distribution of samples taken each year are shown in Table 3. The values for samples taken each year include a successive number (1… n) that reflects the relative sampling height (RSH) with respect to the base of the corridor that runs along the arch barrel. The height difference between two successive samples varied between 55 and 50 cm.

Table 3 Data and values of the arithmetic mean, standard deviation, for salt content (%) of samples taken from 2005 to 2013. RSH = relative sampling height.

2005								
Halite	Thenardite	Konyaite	Nitratine	Humbers.	Arcanite	Aphthitalite	Sylvite	RSH
1	97	0	1	0	1	0	0	1
5	78	1	0	0	0	16	0	2
42	39	1	11	6	1	0	0	3
39	51	1	7	0	1	0	1	4
26	61	1	1	0	0	11	0	5
24	64	0	0	11	1	0	0	6
32	38	1	10	17	1	0	1	7
24	61	1	4	5	0	4	0	8
24.1	61.1	0.7	4.3	4.9	0.6	3.9	0.3	← $\bar{x}$
14.7	19.7	0.5	4.5	6.3	0.5	6.2	0.5	←σ
2008								
Halite	Thenardite	Konyaite	Nitratine	Humbers.	Arcanite	Aphth.	Sylvite	RSH
49	10	9	1	26	2	0	3	1
60	12	6	0	16	1	0	5	2
54	14	0	0	28	1	0	3	3
57	13	0	0	24	1	0	6	4
58	21	17	0	0	2	0	2	5
55	14	6	0	19	0	0	0	6
55.4	13.8	6.5	0.2	18.7	1.2	0	3.2	← $\bar{x}$
3.7	3.9	6.4	0.4	10.2	0.7	0.0	2.1	←σ
2011								
Halite	Thenardite	Konyaite	Nitratine	Humbers.	Arcanite	Aphth.	Sylvite	RSH
41	26	7	0	22	2	0	2	1
43	12	9	3	31	0	2	0	2
44	9	9	4	25	4	1	3	3

52	8	17	6	12	4	0	3	4
51	9	10	4	23	0	1	1	5
68	7	0	3	19	0	1	1	6
77	18	0	1	0	0	1	3	7
77	19	0	0	0	0	0	4	8
56.6	13.7	6.6	2.8	16.5	1.3	0.8	2.1	← $\bar{x}$
15.1	6.8	6.2	2.2	11.4	1.9	0.7	1.3	←σ

2013									
Halite	Thenardite	Konyaite	Nitratine	Humbers.	Arcanite	Aphth.	Sylvite	Darapskite	RSH
8	61	17	0	0	0	12	2	0	1
8	69	0	0	9	0	6	0	8	2
8	66	11	0	5	0	5	0	5	3
60	14	17	0	5	0	4	0	0	4
61	14	8	0	11	0	1	0	5	5
70	16	0	0	10	0	1	0	3	6
58	22	3	0	14	0	0	0	3	7
59	17	6	0	18	0	0	0	0	8
41.5	34.9	7.8	0	9.0	0	3.6	0.3	3.0	← $\bar{x}$
28.0	25.4	6.8	0	5.7	0	4.1	0.7	2.9	←σ

The efflorescence was of various types: mainly powdery, but occasionally presenting whisker morphologies. It was often hardened or had a cemented surface, creating a crust and a discontinuity between the salt crust and the building stone that had been favored by erosion, mainly through flaking.

In 2011, six years after the cleaning process [1] described in the introduction salts appeared as crusts of the order of 10 μ thick and as sub-efflorescence located 20–30 μm away from the surface.

A significant loss of material had occurred following restoration, and in some places, the edges and corners had worn down by more than 1 cm in eight years (Fig. 5). This damage was similar to stage 4 [31] regarding the evolution of very pronounced alveoli; however, in this case it was related to granular disintegration into sand. In some corners of the south side, massive loss of material was observed, generally associated with concave erosion surfaces (arrows).

Fig. 5 Erosion on the corners of the south wall. July 2013.

3.4 Salt mineralogy, 2005

The major component in the samples collected prior to restoration of the bridge was thenardite, which mainly accumulated at low RSH values. The following component abundant in salt phase was halite, which increased with an increase in RSH. Humberstonite tended to accumulate preferably at the top of the vertical profile, and also showed high values, sometimes up to 11%. Aphthitalite and nitratine were also common saline phases in the efflorescence, but with a patchy distribution. Konyaite, sylvite and arcanite showed truly low values, also appearing in a patchy distribution.

3.5 Salt mineralogy, 2008

The spatial distribution of the salt phase in the samples collected in 2008, Table 3, was more homogeneous. Halite was now the major component in all samples, with an average content of up to 55%. Three years after cleaning the bridge, thenardite had become scarce in efflorescence, with mean values of 14%, and it tended to be more abundant in the upper part of the section. The most abundant mineral after halite was humberstonite, with mean values in excess of 18% and showing a slight tendency to accumulate at the bottom of the profile. Also present were konyaite (6%) and sylvite (4%), both presenting a patchy distribution.

3.6 Salt mineralogy, 2011

Halite was also the major component in the samples collected in 2011 (56.6% average), although it tended to accumulate at higher levels, reaching a content of 77% and showing positive correlation coefficients and higher (0.95) values in relation to RSH. Meanwhile, humberstonite, thenardite, and konyaite presented an average content of about 16, 13 and 6%, respectively, and tended to accumulate in lower parts of the area sampled. With an average content of 3%, nitratine (Fig. 6A) accumulated in the middle levels, while arcanite (Fig. 6B), aphthitalite, and sylvite had an average content of between 1 and 2% and showed a patchy distribution (Table 3).

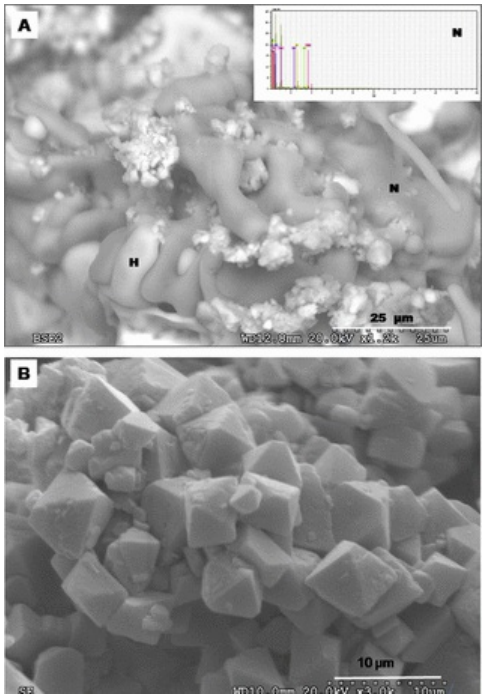

Fig. 6 A. SEM photomicrograph in bse mode of sodium salts and EDS. H halite and N nitratine. B. SEM photomicrograph in se mode of arcanite.

3.7 Salt mineralogy, 2013

The spatial distribution of saline phases in the samples collected in 2013 (see Table 3) was different from that in samples collected in 2008 and 2011, but quite similar to the results obtained in 2005, before salt remove. Thenardite was again the dominant phase in the lower levels, accounting for up to 61%, but decreased in the middle and upper levels. It presented a predominantly fibrous behavior. The distribution of halite was complementary, low at low levels but increasing at middle and high levels, reaching up to 60%. Double salts such as darapskite and aphthitalite (Fig. 7) accumulated in the lower part of the efflorescence, while humberstonite did so in the upper part. The humberstonite distribution is quite similar to 2005 but different to the values obtained in 2008 and 2011 (Table 3).

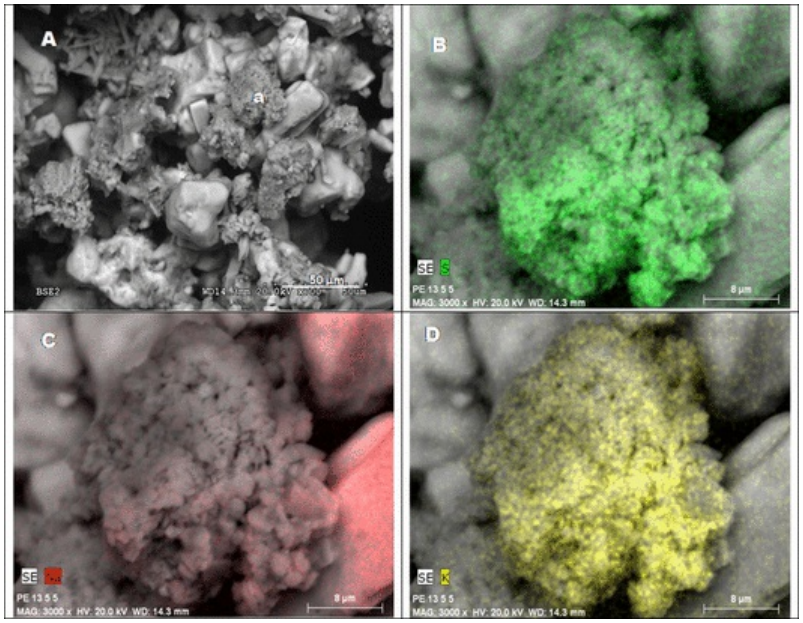

Fig. 7 Aphtitalite. A SEM photomicrograph in se mode (an aphtitalite aggregate) B, C and D some element distribution (B: Sulfur; C: sodium; D potassium).

3.8 Soluble anions and cations in the soil near the bridge abutment

Soil sampling was done on the slope next to the bridge abutment, where efflorescence and salt crusts had been identified. The slope was formed by building demolition rubble, and fragments of walls and gypsum plasters were identified by visual inspection. Samples were taken in a sample tube with an external diameter of 2 cm and a length of 30 cm. Sampling points, numbered down slope (Table 4), were positioned along a profile located 50 cm from the abutment, in the perpendicular direction to the river. Samples were studied by ion chromatography following the procedure described in the methodological section above. The prevailing ions in solution were Ca^{2+} and SO_4^{2-}. The Cl^-/NO_3^- relationship decreased towards the upper part of slope, with values close to 1.6, implying an increase in nitrates. Meanwhile, Na^+/K^+ showed no similar trends in variation trends and values ranged from 2.7 to 4.7 (Table 5).

Table 4 Data for soluble anions and cations in soils. Samples taken downwards (1–4) on the landfill demolition, located on the left abutment.

	Sample 1	Sample 2	Sample 3	Sample 4
Anions (meq/l)				
Cl^-	2.38	2.28	2.40	1.43
NO_3^-	1.49	0.84	0.83	0.36
SO_4^{2-}	17.51	17.14	7.34	20.48
Σanions (eq.)	21.37	20.27	10.56	22.27
Cations (meq/l)				
Na^+	3.15	3.15	3.80	2.61
Ca^{2+}	24.34	19.63	8.73	24.67
K^+	0.79	1.15	0.82	0.67

Σcations (eq.)	28.-28	28.-28	13.-34	27.-95

Table 5 Monthly variation in [RHmaximun (%) – RHmínimun (%)]/RHaverage] referring to the RH value. Data from: "Climatic data for Elche, 2000–2014, from the Elx EEA SIAR meteorological station".

Month	Maximum RH (%)	Minimum RH (%)	Average RH (%)	Δ RH monthly/RH average
1	95.68	19.86	63.7	1.19
2	96.05	16.88	61.88	1.28
3	96.53	17.02	61.7	1.29
4	96.25	17.03	61.15	1.3
5	95.56	18.07	61.1	1.27
6	93.44	17	59.77	1.28
7	93.59	16.74	63.11	1.22
8	93.61	17.54	64.05	1.19
9	94.91	19.93	66.12	1.13
10	96.19	21.79	68.1	1.09
11	96.53	22.35	63.94	1.16
12	96.62	23.49	64.47	1.13

4 Discussion

4.1 Geochemistry and physical chemistry of minerals

The mineralogy identified in samples collected from the profiles sampled between 2005 and 2013 varied in the vertical profile, and varied greatly between years, especially after restoration work involving the removal of efflorescence and salt crusts in 2005. Samples collected in the last year (2013) presented a very similar mineralogical nature and distribution to those taken prior to restoration in 2005. Many types of salts were identified in the efflorescence sampled between 2005 and 2013. These included very common and abundant simple salts, such as halite and thenardite, and other less common or abundant simple salts, such as nitratine and sylvite. Double salts such as Na sulfate-sodium nitrate (darapskite), Na-Mg sulfate salts (konyaite), and K-Mg sulfate salts (aphthitalite) were also found, together with perhaps the most abundant double salt identified in the efflorescence studied here, also a K-Na-Mg sulfate-nitrate (humberstonite).

Recently, Linnow et al. [32] reported that double salts had been detected in building materials, and that most of these salts were incongruently soluble compounds, and also indicated that in contrast to simple salts, no systematic research has been conducted on the behavior and effects of double salts on building materials. They obtained a sequence of metastable Na_2SO_4 phases and darapskite, comparable with observations made on Andean nitrates [15]. Likewise Linnow et al. [32] points the influence of RH (atmospheric relative humidity) on the nature of the salts $NaNO_3$-Na_2SO_4-H_2O, and also observed aphthitalite formation when potassium sulfate was added to the previous thermodynamic system [33].

Below, we highlight some of the mineralogical aspects of some of the double salts identified in the efflorescence collected from the left abutment of the bridge at Elche.

4.2 The physical and physical-chemical processes involved in the genesis of efflorescence and salt crusts

Sodium sulfate (thenardite) and sodium chloride (halite), the most abundant mineral phases in the efflorescence studied here, are two common salts identified as causing the deterioration of porous rocks, and this has been well-documented [34]. The intensity of damage induced by both salts may be related to a crystallization-dissolution mechanism. The weather also plays a major role in the deterioration of building materials, due to "phase transitions from anhydrous phases to poorly hydrated ones, and […] the influence of these phase transitions caused by annual variations in relative humidity (RH)" [35,36]. However, the kinetics of hydration, dehydration, and deliquescence are only strongly affected by porosity, when the pore-filling ratio of salt and solution is so high that the effectiveness of vapor transport is reduced [37]. Similarly, a thermodynamic model capable of predicting the crystallization behavior of salt mixtures as a tool to predict environmental conditions and minimize salt damage has been introduced [38].

4.2.1 Imbibition or capillary waters, and solute origin

Water can enter a porous material either as liquid or vapor [39]. In the liquid state, two mechanisms may operate: capillarity and/or infiltration. Capillary water height in the walls can be modeled as the height (h) of the ascending liquid in a capillary, as it is well know:

$$H = \frac{2S_{LV}\cos\theta}{\rho g r}$$

This height is a function of surface tension, S_{LV}, which is related to the saline concentration in water; S_{LV} values can be calculated as described by Leroy et al. [40]. The contact angle (θ) increases with increasing electrolyte concentration, and the relationship is non-linear [41]. ρ is the fluid density. Dynamic viscosity (η) increases at higher concentrations [42]. The capillary radius, r, is an estimator of pore system functioning and g is the value of gravitational acceleration. In our case, the capillary height measured in masonry walls ranged from 2 m to 2.5 m, mainly along an old masonry wall embedded in the abutment of the bridge, and along the mortar joints in the belt course and in the random rubble masonry just below. These values are close to those reported by Martínez-Martínez et al. [43].

The foundations of the bridge stand on loose silt and sand sediments that locally include some gravel deposits, probably a river terrace (+9 m), on which a paleosol has formed with carbonate crusts. Hydro-geologically speaking, these deposits belong to the "*Campo de Elche* Shallow Quaternary Aquifer". This is an unconfined aquifer with piezometric levels located at depths of 1–3 m. From a hydrochemical point of view, the aquifer displays a homogeneous composition of hydrochemical facies (Piper diagrams) with a high sodium chloride component, much lower concentrations of sulfate and bicarbonate, and high conductivity values sometimes in excess of 10,000 μS/cm in the central sector [44].

The equilibrium profile between liquid water and water vapor (a_w/p_w) in the wall section is given by the equation $\xi = k\, p_w(a_w - RH/100)$, where ξ is the evaporation (+)/condensation (–) ratio, k is the mass transfer coefficient (Dalton's equation), related among other factors to wind speed, p_w, is the water pressure in equilibrium with the air, a_w is the water activity of the liquid water at the wall, and RH is the relative humidity [45,46]. Therefore, for values of a_w < RH, before water imbibition, evaporation occurs, and saturation may be reached in saline phases. These salt phases may accumulate approximately parallel to the contact between the porous material and air (sub-efflorescence, efflorescence or salt crusts) in more or less discontinuous salt levels.

The evaporation processes described and the chemical composition of groundwater explain the presence of the most common efflorescence salts on the bridge, halite and thenardite. However, our observations show that trends in the vertical distribution of salts changed over the years, especially as regards thenardite, and the same may be said for humberstonite. Furthermore, they cannot explain the presence and vertical distribution of nitrates, especially double salts such as darapskite and humberstonite. Thus, for the mineral darapskite to be thermodynamically stable, the relationship $NaNO_3/Na_2SO_4$ in evaporation front must exceed 0.7 [47,48]. The data available on nitrate content of groundwater show that it exceeds 50 ppm [49], and therefore capillary water evaporation alone does not explain the salts identified in the salt crusts and efflorescence.

We cannot discard rule out the possible influence of water percolating through the building demolition rubble (mainly calcium sulfate composition) located on the slope on the sampled side of the bridge (see Table 4 for explanation), which would contribute sulfate and calcium ions to water imbibition. Similarly, it may also contribute nitrates, but in this case the $NaNO_3/Na_2SO_4$ ratio values were also so low (see Table 4) to reach saturation in double nitrate ~~sulphates~~ sulfates salts as will be seen later. Although infiltration waters from rainwater and street wash waters were not considered in this study, it is worth noting that the salt crusts located on the intrados of the keystone were mainly formed by thenardite, with minor amounts of syngenite [50].

4.2.2 Water vapor condensation [(RH/100)] > a_w) and PM (particulate matter in the air)

The transition between liquid water and water vapor is the dew point of water vapor defined by the equation RH = a_w. As mentioned above, water condensation is related to the RH/a_w ratio, and variations in RH affect this equilibrium. RH variation is related to: a) the absolute moisture content of the air at all times, which varies according to the weather; b) diurnal temperature fluctuations, under constant conditions of water vapor content in the air; and c) breezes from the coast, in areas near the sea. Annual RH variation in Elche, calculated as the mean difference between extreme monthly average values ([RHmaximun (%) – RHmínimun (%)]/RHaverage) ~~.~~ which are considerably higher than the daily average values ~~.~~ shows coefficient of variation (CV) values below 6%.

Given the wide variations in the monthly average RH, the absolute value of which differed little from daily average variations, these variations in RH can be considered a basic factor in daily moisture/dryness cycles in the walls.

Meanwhile, the other factor relationship, a_w, varies according to:

a) The surface roughness of walls, an effect known as the Lotus Effect and described by Philip [51], this work furnished a quantitative basis for analyzing combine adsorption and capillary condensation on rough surfaces, and is not take in account in this paper.

b) The porosity of building materials (pore water system), such that variation in log a_w may be expressed as log $a_w = -(0.000921/2r)$, where r (μm) is an estimation of pore radius [52–54] and explains capillary condensation in nanopores due to spontaneous formation of ordered water structures which are energetically favored. Similarly, the effect of grain size can be described, whereby fine grains tend to hold more moisture than coarse ones see [55].

c) Salts, which can also absorb moisture, especially when relative humidity increases above their DRH (deliquescence relative humidity) equilibrium in the eutectic point [56,57]. Very soluble salts may then deliquesce, i.e. absorb so much water that they form a saturated solution [(RH/100)] > a_w) (eutectic point in a single salt solution). To establish the stability of the salts with regard to DRH, it was necessary to calculate the values of a_w at the eutectic point for each salt. As stated in the caption to the Table 6, some of the DRH data, have been taken from Grassegger and Schwartz (2008) [30] and corrected and supplemented with other data published [58]. When data is unavailable, DRH values have been estimated by calculating a_w in single salt saturated solutions: i) From the solubility data of the simple salt, calculating the saturated

molality bibliographic data from the solubility of the salt solution; ii) When the solubility data, the thermodynamic data of the salt is not known, solubility values were computed for each salt, estimated from the standard free energy, ΔG^0_f, using the method described by Golan Mostafa et al. [59]. Then, a congruent dissolution was considered and the values of free energy change, ΔG^0_{disol}, were calculated. Using the values of each ion ΔG^0_f, as tabulated by Wagman et al. [60], it was possible to estimate the a_w, in solution at equilibrium (DRH). The behavior of a single salt at a given temperature can be sufficiently characterized by a single value of DRH. If the humidity remains above this RH the salt remains dissolved, however, if it drops below the DRH the salt will crystallize [12] (Table 7).

able 6 DRH values for the different single salts identified for the different single salts identified in the efflorescence and saline crust. ∗) Estimated from solubility values, see text; ∗∗) Data from: Grassegger and Schwartz (2008) [30], ∗∗) corrected and supplemented with other data published [58].

Mineral	DRH (%)
Darapskite	67.6∗
Nitratine	74.2∗∗
Halite	75.3∗∗
Humberstonite	77.8∗
Sylvite	84.3∗∗
Thenardite	86.9∗∗
Konyaite	88.7∗
Aphthitalite	91.2∗
Arcanite	97.3∗∗

able 7 Chemical composition of particulate matter (data from Nicolas et al. [3]), and the equivalent fractions for nitrate/sulfate and sodium/magnesium calculated from data. PM2.5: Suspended particulate matter with a diameter less than 2.5 μ. PM10: Suspended particulate matter with a diameter less than 10 μm.

PM2.5		
Anions (μg m^{-3})	Mean	SD
Cl^-	0.18	0.22
NO_3^-	1.37	2.21
NH_4^+	1.63	1.4
SO_4^{2-}	3.79	2.92
ΣN/ΣN + S	0.58	
Cations (μg m^{-3})	Mean	SD
Na^+	0.27	0.11
Ca^{2+}	0.36	0.16
Mg^{2+}	0.02	0.01
K^+	0.21	0.16

$Na^+/(Na^+ + Mg^{2+})$	0.86	
PM10		
Anions (μg m^{-3})	Mean	SD
Cl^-	0.60	0.5
NO_3^-	3.76	2.99
NH_4^+	1.10	1.19
SO_4^{2-}	4.36	3.09
$\Sigma N/\Sigma N + S$	0.57	
Cations(μg m^{-3})	Mean	SD
Na^+	0.99	0.72
Ca^{2+}	2.29	0.98
Mg^{2+}	0.16	0.1
K^+	0.28	0.26
$Na^+/(Na^+ + Mg^{2+})$	0.77	

The results obtained show that the salts with DRH values below that of halite may redissolve almost daily, which can substantially modify the precipitation sequence of salts related to previous salts from water imbibitions or capillaries. Such damage is the result of crystallization pressure, which causes material fatigue due to the high frequency compression-decompression cycles associated with crystallization-dissolution. This frequency can be seen daily in climates such as that of Elche, with strong diurnal variations in RH, lading to salt efflorescence with minerals of lower DRH (deliquescence relative humidity) values. This is probably one of the most important factors in the evolution of saline efflorescence minerals, and in the analysis of the damage to the stone materials induced by salt crystallization-solution processes.

These effects of variation of the RH, minerals phases on the salt efflorescence, is amplified by the fact that efflorescence are salt mixtures. Described to the RH salt mixtures influence on behavior, it is required to define RH range. RH The upper limit depends on mixture composition, the RH limit is given by the relative humidity in equilibrium a salt mixture saturated solution. The upper RH limit depends on mixture composition, the RH limit is given by the relative humidity in equilibrium with the solution that is saturated in both solids. This relative humidity is called the mutual DRH (MDRH). "*The MDRH is always lower than the DRH of any single salt in the mixture* [12,56,57,61,62].

These cycles of crystallization–condensation on efflorescence, allow the incorporation of atmospheric particulate matter, which can be trapped (trapping effect) in the exterior of efflorescence, particularly in the walls most exposed to the wind, in this case, the south wall affected by the prevailing winds.

Nicholas et al. [3] determined the composition of atmospheric particles, revealing that the secondary inorganic compounds NH_4NO_3 and $(NH_4)_2SO_4$ were the major components of the fine fraction, representing 40% of the total mass. In the coarse fraction, $NaNO_3$ and $Ca(NO_3)_2$, $CaCO_3$ and NaCl accounted for nearly 50% of the measured mass. These authors indicated the seasonal evolution, as a consequence of the influence of the sea-breeze, of the precipitation rate and the temperature, which affected vehicle- and wind-induced re-suspension of dust. The sodium (Eq. –%), related to $Mg^{2+} = Na^+/(Na^+ + Mg^{2+})$, and nitrate (Eq. –%) related to $SO_4^{2-} = \Sigma N/(\Sigma N + S)$ was calculated from data obtained by Nicolas et al. [3], and provided an explanation for the presence of nitrates in the efflorescence.

4.2.3 The genesis of double salts within efflorescence and relative humidity (DRH and MDRH)

Theoretical considerations and numerical approaches have revealed the important role of RH in the development and evolution of salts [47] (Fig. 8). In a saline solution similar to that described in Fig. 8, when sodium equivalents predominate over magnesium as the RH decreases due to evaporation, the first event is precipitation of mirabilite (Na_2SO_4.10H2O); mirabilite is then joined by bloedite at about MDRH ≈ 80%. Subsequently, mirabilite is replaced by the water-free sodium sulfate, thenardite (Na_2SO_4), which is replaced by the double salt darapskite ($Na_2SO_4{\cdot}NaNO_3{\cdot}H_2O$). At an RH ≈ 72%, darapskite and bloedite can coexist. As is evident from the precipitation paths, different salts may crystallize simultaneously over a wide range of humidity values.

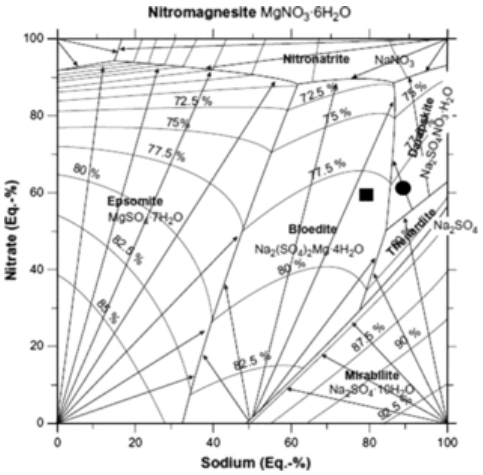

Fig. 8 Projection from $RH_{\_}$(%) in the Na-Mg-SO_4-NO_3-H_2O system, phase diagram after Franzen & Mirwal (2009) [51]. Hairlines represent RH isobars; arrows show evolution path of solution during drying. Graphic symbols used: PM 2.5, circle; PM10, squares.

From the data given in Table 1 and shown in the phase diagram in Fig. 8, it can be seen that the soluble ions in PM 2.5 particles are in the stability field of darapskite while in PM10 particles, they are in the stability field of bloedite, probably in a less hydrated form as konyaite. As evaporation intensified, both reached the bloedite (konyaite)–darapskite equilibrium line, to finally precipitate in the eutectic point of bloedite (konyaite)–darapskite–nitratine, at which point the environmental RH was below 72.5%.

This agrees with the observations on Andean saline deposits [25,28]. They defined two basic types of brine: a) Na-brines trend, in which the precipitation sequence is: glauberite-darapskite-(halite nitratine); and b) Na-Mg-K brines trend, where the precipitation sequence is bloedite (konyaite)-humberstonite-(halite-nitratine). The presence of halite-nitratine saline phases associated with the eutectic point may be interpreted as evidence of the existence of incongruent dissolution processes of preexistent double salts (such as darapskite or humberstonite), enabling precipitation of new simple minerals (nitratine, halite, sylvite and arcanite) in the hollows of the residual porosity. The humberstonite would be formed under the same conditions as the darapskite, as indicated by Vega et al. [14]. These authors hypothesized that the presence of Mg^{2+} and K^{+1} in the environment leads to the formation of a bloedite sequence: konyaite (pentahydrate phase of similar composition to bloedite) > humberstonite > halite > nitratine. Moreover, increasing the relative humidity can destabilize the previous phases, which are deliquescent salts appearing as mirabilite that evolve into thenardite at lower RH values., and which may entail migration to the lower parts of the efflorescence profile “per descensum”. In the absence of hydrated phases at ambient temperatures and at a RH below 75.3%, dissolved an RH below 0.78, dissolved halite may rise by capillarity and concentrate in the upper part of the efflorescence profile, in accordance with our observations on the vertical distribution of minerals. This process is repeated almost daily, due to sudden changes in environmental RH.

5 Conclusions

The location of salts in the walls was determined by a balance between two diffusive processes, the evaporation-condensation of air in contact with the wall and the capillary flow of charged ions in water solution. Evidently, variations in environmental conditions can cause a particular salt to crystallize as efflorescence or sub-efflorescence at different times (diurnal and seasonal scale), generally forming “stratigraphic sequences” of salts of the same nature.

According to our data, the mineralogy of the efflorescence varied significantly over the nine years studied, both in terms of abundance and vertical distribution. Abundance and nature varied from year to year. Thus, the predominant mineral before restoration (Table 3) was the thenardite, followed by halite, and occasionally appreciable amounts of humberstonite and nitratine. In the samples taken in 2008 (Table 3), immediately after restoration, the dominant mineral was halite, while humberstonite considerably exceeded thenardite, and appreciable amounts of konyaite appeared. In 2011 (see Table 3), halite continued to form the dominant mineral, and humberstonite continued predominate over thenardite. In 2013 (see Table 3) the predominant mineral was again halite, but there was also a strong presence of thenardite, and significant amounts of humberstonite and konyaite.

The ions present in capillary water mainly came from a mixture of groundwater and seepage waters. The chemical composition of the groundwater showed a high sodium chloride component and much lower concentrations of sulfate and bicarbonate, which explained the presence of halite, while seepage water next to the wall was related to leaching of gypsiferous demolition rubble, and might explain the presence of sulfate salts, thenardite, konyaite, aphthitalite, and arcanite.

The low MDRH (Mutual Deliquescence Relative Humidity) and DRH (Deliquescence Relative Humidity) values of some of the single salts and mixtures, in the efflorescence, explain the processes of “trapping” atmospheric dust and subsequent incorporation of the ions into the saline solution. It is also interesting to note the similarity between the mineral assemblages of saline efflorescence on the Old Bridge and those of the Andean salt flats, in terms of precipitation sequences and SEM textures.

The less soluble salts with higher DRH values developed specific crystalline idiomorphic habits (SEM), while more soluble salts with the lowest DRH values, such as halite and nitratine, exhibited “surface dissolution textures”. Also

notable was the occasional presence of thenardite (XRD) with a fibrous habit (SEM), a pseudomorph from mirabilite.

The salt mineralogy of the efflorescence varied over time, but in general, the present mineralogical composition is similar to that identified prior to cleaning and restoration of the bridge nine years ago.

6 Final considerations and recommendations

Restoration of the bridge and removal of efflorescence (2005), and even replacement of fill material and waterproofing treatments, has not prevented the development of efflorescence on the abutment in a relatively short time (nine years). This is because the chemical composition of the waters at the foundations, climatic characteristics and the mineralogical nature of airborne particulate matter have not changed. Consequently, the cleaning process may have contributed to creating new surfaces that are exposed to environmental action, increasing the intensity of weathering processes and erosion of stones and mortar joints. Thus, although the restoration works were correct, the only long-term result has been the virtual disappearance of water infiltration efflorescence on the arch barrel.

Acknowledgements

The research activity is partially developed within the Geomaterials Programme (S2013/MIT-2914), founded by the Regional Government of Madrid. We thank the suggestions of editor Prof. Forde, and anonymous referees that improved our manuscript.

References

[1]

M. Louis, M.A. García del Cura, A. Bernabéu, A. La Iglesia, Y. Spairani, J.A. Huesca and R. Prado, The Restoration of a stone bridge in semiarid environment: Puente Viejo of Elche (SE Spain), In: Fort, Alvarez de Buergo, Gómez-Heras and Vazquez Cal, (Eds.), *Heritage, Weathering & Conservation* **vol. 2**, 2006, Taylor & Francis Group; London, 881–885, Balkema.

[2]

S. Ordóñez, M.A. García del Cura, R. Fort, M. Louis, M.C. Lopez De Azcona and F. Mingarro, Physical properties and petrographic characteristics of some Bateig stone varieties, In: *7th Congress of Int. Association of Engineering Geology. V,* 1994, 3595–3603.

[3]

J.F. Nicolas, N. Galindo, E. Yubero, C. Pastor, R. Esclapez and J. Crespo, Aerosol inorganic ions in a semiarid region on the southeastern Spanish Mediterranean COSAT, *Water Air Soil Pollut.* **201**, 2009, 149–159.

[4]

C. Gagnaison, C. Montenat, J. Moratalla, P. Pierre Rouillard and E. Truszkowski, Une ébauche de sculpture ibérique dans les carrières de la Dame d'Elche, *Le buste d'El Ferriol (Elche, Alicante) Mélanges de la Casa de Velázquez Nouvelle série* **36** (1), 2006, 153–172.

[5]

M.P. Luxan, J.L. Prada and J. Borrego, Dama de Elche: pigments, surface coating and stone of the sculpture, *Mater. Struct.* **38**, 2005, 419–424.

[6]

B Fitzner and K Heinrichs, Photo Atlas of Weathering Forms on Stone Monuments, 2004, http://www.stone.rwth-aachen.de (14/04/2015).

[7]

D. Costa and J. Delgado Rodrigues, Desalinization of granite surfaces with silica sols. In situ evaluation of their efficacy when applied to decayed materials, In: *In Salt Weathering on Buildings and Stone Sculptures,* Proc. Int. Conference, Copenhagen, 20082008, Technical University of Denmark, 317–327.

[8]

F. Gázquez, F. Rull, J. Medina, A. Sanz-Arranz and C.C. Carlos Sanz, Linking groundwater pollution to the decay of 15th-century sculptures in Burgos Cathedral (northern Spain), *Environ. Sci. Pollut. Res.* (22), 2015, 15677–15689, http://dx.doi.org/10.1007/s11356-015-4754-6.

[9]

Y. Matsukura, C. Oguchi and N. Kuchitsu, Salt damage to brick kiln walls in Japan: spatial and seasonal variation of efflorescence and moisture content, *Bull. Eng. Geol. Env.* **63**, 2004, 167–176, http://dx.doi.org/10.1007/s10064-003-0211-8.

[10]

H. Morillas, M. Maguregui, C. Paris, L. Ludovic Bellot-Gurlet, P. Colomban and J.M. Madariaga, The role of marine aerosol in the formation of (double) sulfate/nitrate salts in plasters, *Microchem. J.* **123** (2015), 2015, 148–157, http://dx.doi.org/10.1016/j.microc.2015.06.004}.

[11]

K. Zehnder and A. Arnold, Crystal growth in salt efflorescence, *J. Cryst. Growth* **97** (2), 1989, 513–521, http://dx.doi.org/10.1016/0022-0248(89)90234-0.

[12]

M Steiger and A.E. Charola, Weathering and Deterioration, 227–316, In: S Siegesmund and R. Snethlage, (Eds.), *Stone in Architecture Properties, Durability,* 2011, Springer-Verlag; Berlin Heidelberg, 551 p.

[13]

A.E. Charola and C. Bläuer, Salts in masonry: an overview of the problem, *Restorat. Build. Monuments* **21** (4–6), 2015, 119–135.

[14]

G.E. Ericksen and M.E. Mrose, Mineralogical studies of the nitrate deposits of Chile. II. Darapskite, Na3(NO3)(SO4)·H2O, *Am. Mineralogist* **55**, 1970, 1500–1517.

[15]

M. Vega, G. Chong and J.J. Pueyo, Parental brine evolution in the Chilean nitrate deposits (Pedro de Valdivia, II Región de Antofagasta), Mineralogical and Petrographic data, 1996, Third ISAG; S1 Malo (France), (17–19/9/1996, pp. 707–710).

[16]

C.T. Oguchi, Y. Matsukura, H. Shimada and N. Kuchitsu, Application of water susceptibility index to salt damage in a brick monument, In: Fort, Alvarez de Buergo, Gómez-Heras and Vazquez Calvo, (Eds.), *Heritage, Weathering & Conservation* **vol. 2**, 2006, Taylor & Francis Group; London, 881–885, (Balkema 217–227).

[17]

A. Shayan and C.J. Lancucki, Konyaite in salt efflorescence from a Tertiary marine deposit near Geelong, Victoria, Australia, *Soil Sci. Soc. Am. J.* **48**, 1984, 939–942.

[18]

C.K. Kohut and M.J. Dudas, Evaporite mineralogy and trace-element, *Can. J. Soil Sci.* **73**, 1993, 399–409.

[19]

B.J. Buck, J. King and V. Etyemezian, Effects of salt mineralogy on dust emissions, Salton Sea, California, *Soil Sci. Soc. Am. J.* **75**, 2011, 1971–1985.

[20]

H.S. Washington and H.E. Merwin, Aphthitalite from Kilauea, *Am. Mineral.* **6**, 1921, 121–125.

[21]

V.R.K.S. Susarla, K.M. Chudasama, V.P. Mohandas and P.K. Ghost, Glaserite preparation by sodium sulfate and potassium chloride, *J. Sci. Ind. Res.* **66**, 2007, 444–449.

[22]

A.E. Charola, L. Lazzarini, G.E. Wheeler and R.J. Koestler, The Spanish Apse from San Martin de Fuentidueña at the Cloisters, In: *Preprints of the Inter. Inst. Conser. Hist. Art. Works, Bologna,* 1986, Metropolitan Museum of Art; New York, 18–21.

[23]

M.E. Mrose, J.J. Fahey and G.E. Ericksen, Mineralogical studies of the nitrate deposits of Chile. III. Humberstonite, K3Na7Mg2(SO4)6(NO3)2·6H2O, a new saline mineral, *Am. Mineral.* **55**, 1970, 1518–1533.

[24]

K. Cai, J. Gao, D. Dejun Zhao and Y. Yu, Mineralogical studies of humberstonite and darapskite in Luobubo region, China, *Acta Mineral. Sin.* **12** (2), 1992, 143–151.

[25]

R.A. Howley and D.L. Shettel, Tachyhydrite and Other Soluble Salts: Relevance to the Proposed Nuclear Waste Repository at Yucca Mountain, Nevada, 2004, Nuclear Waste Project Office Agency for Nuclear Projects State of Nevada Carson City, 30 p.

[26]

J.J. Pueyo, G. Chong and M. Vega, In: *Mineralogía y evolución de las salmueras madres en el yacimiento de nitratos Pedro de Valdivia* **vol. 25**, 1998, Revista Geológica de Chile; Antofagasta, Chile, 3–15.

[27]

G.E. Ericksen, Geology and origin of the Chilean nitrate deposits: USGS Professional Paper 1188, 1981, 37p..

[28]

G.E. Ericksen, The Chilean nitrate deposits, *Am. Sci.* **71**, 1983, 366–374.

[29]

Y.Z. Chen, C.L. Liu, P.C. Jiao and J.M. Han, Preliminary Researches on Nitrate Formation by Metal-Catalyst Photochemical Reaction in Arid Region of Xinjiang; Mineral Deposits; 2009–05, 2009, http://en.cnki.com.cn/Article_en/CJFDTOTAL-KCDZ200905018.htm.

[30]

G Grassegger and H.-J. Schwarz, Salze und Salzschäden an Bauwerken, In: H.-J. Schwarz and M Steiger, (Eds.), *Salzschäden an Kulturgütern,* Stand des Wissens und Forschungsdefizite Ergebnisse des DBU Workshops in February, 2008 in Osnabrück2008, 6–21.

[31]

E. Rothert, T. Eggers, J. Cassar, J. Ruedrich, B. Fitzner and S. Siegesmund, Stone properties and weathering induced by salt crystallization of Maltese Globigerina Limestone, In: R. Prikryl and B.J. Smith, (Eds.), *Building Stone Decay: From Diagnosis to Conservation* **271**, 2007, Geological Society, London, Special Publications, 189–198.

[32]

K. Linnow, M. Steiger, C. Lemster, H. Clercq and M. De Jovanović, In situ Raman observation of the crystallization in $NaNO_3$–Na_2SO_4–H_2O solution droplets, *Environ. Earth Sci.* **69** (5), 2012, 1609–1620.

[33]

H.De. Clercq, M. Jovanovic, K. Linnow and M. Steiger, Performance of limestones laden with mixed salt solutions of Na_2SO_4–$NaNO_3$ and Na_2SO_4–K_2SO_4, *Environ. Earth Sci.* **69**, 2013, 1751–1761.

[34]

N. Shahidzadeh-Bonn, F. Bertrand and D. Bonn, Damage in porous media due to salt crystallization, *Phys. Rev. E* **81**, 2010, 066110, Published 16 June 2010.

[35]

E.M. Ruiz Agudo, Prevención del daño debido a la cristalización de sales en el Patrimonio Histórico Construido mediante el uso de inhibidores, (PhD Thesis)2007, Granada University, 351 pp..

[36]

C.M. Grossi, P. Brimblecombe, B. Menéndez, D. Benavente, I. Harris and M. Déqué, Climatology of salt transitions and implications for stone weathering, *Sci. Total Environ.* **409**, 2011, 2577–2585.

[37]

R.M. Espinosa, L. Franke and G. Deckelmann, Phase changes of salts in porous materials: crystallization, hydration and deliquescence, *Constr. Build. Mater.* **22**, 2008, 1758–1773.

[38]

A.E. Charola and Herodotus, Salts in the deterioration of porous materials: an overview, *JAIC* **39** (3), 2000, 327–343.

[39]

O. Ozdemir, S. Karakashev, V. Anh, A.V. Nguyen and J.D. Miller, Adsorption and surface tension analysis of concentrated alkali halide brine solutions, *Miner. Eng.* **22**, 2009, 263–271.

[40]

P. Leroy, A. Lassin, M. Azaroual and L. Andre, Predicting the surface tension of aqueous 1:1 electrolyte solutions at high salinity, *Geochim. Cosmochim. Acta* **74** (19), 2010, 5427–5442.

[41]

D.A.L. Leelamanie and J. Karube, Soil-water contact angle as affected by the aqueous electrolyte concentration, *Soil Sci. Plant Nutr.* **59**, 2013, 501–508.

[42]

A. Melinder, Thermophysical properties of aqueous solutions used as secondary working fluids, (Doctoral Thesis)In: 2007, School of Industrial Engineering and Management, Royal Institute of Technology, KTH; Stockholm, Sweden, 144 p.

[43]

J. Martínez-Martínez, A. Bernabéu, D. Benavente and M.A. García-del-Cura, Stone decay in civil heritage constructions due to salt crystallization: Salinetes Bridge (Alicante, SE Spain), In: *Water and Cultural Heritage,* 7th International Symposium on the Conservation of Monuments in the Mediterranean Basin. June 6–9 Orleans. 2007**vol. 1**, 2007, 278–286.

[44]

L. Moreno Merino, E. Sánchez Sánchez, G. Ramos González and L. Rodríguez Hernández, Caracterización de los acuíferos del sector meridional de la provincia de Alicante Destinados a desalación para osmosis inversa, In: *VII Simposio de Hidrogeología,* 2001, Asociación Española de Hidrología Subterránea; Murcia, 453–466, http://aguas.igme.es/igme/publica/sim_hidro_murcia.htm (12/05/2015).

[45]

S. Sánchez-Moral, S. Ordóñez, D. Benavente and M.A. García del Cura, The water balance equations in saline playa lakes: comparison between experimental and recent data from Quero Playa Lake (central Spain), *Sed. Geol.* **148** (1–2), 2002, 221–234.

[46]

P. Gamazo, S.A. Bea, M.W. Saaltink, J. Carrera and C. Ayora, Modeling the interaction between evaporation and chemical composition in a natural saline system, *J. Hydrol.* **401**, 2011, 154–164.

[47]

C.W. Franzen and P.W. Mirwald, Moisture sorption behavior of salt mixtures in porous stone, *Chem. Erde* **69**, 2009, 91–98.

[48]

Aqueous Solutions Aps (2015) The NaNO3-Na2SO4-H2O system. EXTENDED UNIQUAD http://www.phasediagram.dk/ternary/ternary1.htm (12/05/15).

[49]

Ministerio de Medio Ambiente, Programa Agua. Seguimiento del Plan Hidrológico de Cuenca del Júcar. Documento de Síntesis, 2007, Oficina de Planificación Hidrológica, 138 p.

[50]

A. La Iglesia, M. Louis, A. Bernabéu and M.A. García del Cura, Eflorescencias salinas en monumentos en clima semiárido: el Caso del Puente Viejo de Elche (Alicante), *Macla* **3**, 2005, 115–116.

[51]

J.R. Philip, Adsorption and capillary condensation on rough surfaces, *J. Phys. Chem.* **62** (12), 1978, 1371–1385.

[52]

Y. Tardy and D. Nahon, Geochemistry of laterites, stability of Al-goethite, Al-hematite, and F^{+3}-kaolinite in bauxites: and approach to the mechanism of concretion formation, *Am. J. Sci.* **285**, 1985, 865–903.

[53]

S. Ordóñez, Petrofísica: aspectos generales, In: F. Mingarro, (Ed), *Degradación Y Conservación Del Patrimonio Arquitectónico,* 1996, 193–212.

[54]

E. Wendler and A.E. Charola, Water and its Interaction with Porous Inorganic Building Materials. Hydrophobe, In: *5th International Conference on Water Repellent Treatment of Building Materials* 2008, Aedificatio Publishers, 57–74.

[55]

J. Coupland, An Introduction to the Physical Chemistry of Food, 2014, Springer, 182 pp.

[56]

R.T. Pabalan, L. Yang and L. Browning, Effects of salt formation on the chemical environment of drip shields and waste packages at the proposed nuclear waste repository at Yucca Mountain, 2002, Report to the U. S. Nuclear Regulatory Commission, CNWRA 2002–3; Nevada, 38 p.

[57]

R.T. Pabalan, Thermodynamic Model of the In-Drift Chemical Environment of a potential High-Level Nuclear Repository Using OLI Software. 23rd OLI Users Conference Parsippany, New Jersey, October, 5–6, 2005.

[58]

Anonymous, In-Drift Precipitates/Salts Model ANL-EBS-MD-000045 REV 03 March 2007, http://pbadupws.nrc.gov/docs/ML0907/ML090770166.pdf (4/01/2016), 2007.

[59]

A.T.M Golam Mostafa, J.M. Eakman and S.L. Yarbro, Prediction of standard heats and Gibbs free energies of formation of solid inorganic salts from group contributions, *Ind. Eng. Chem. Res.* **34**, 1995, 4577–4582.

[60]

D.D. Wagman, W.H. Evans, V.B. Parker, R.H. Schumm, I. Halow, S.M. Bailey, K.L. Churney and R.L. Nuttall, The NBS tables of chemical thermodynamic properties, *J. Phys. Chem. Ref. Data.* **11**, 1982, 1–390.

[61]

D. Gupta, H. Kim, G. Park, X. Li, H.-J. Eom and C.-U. Ro, Hygroscopic properties of NaCl and $NaNO_3$ mixture particles as reacted inorganic sea-salt aerosol surrogates, *Atmos. Chem. Phys.* **15**, 2015, 3379–3393, http://dx.doi.org/10.5194/acp-15-3379-2015, www.atmos-chem-phys.net/15/3379/2015/.

[62]

S. Miroslaw, M.S. Gruszkiewicz, D.A. Palmer, R.D. Springer, P. Peiming Wang and A. Anderko, Phase Behavior of Aqueous Na–K–Mg–Ca–Cl–NO_3 Mixtures: Isopiestic Measurements and Thermodynamic Modeling, In: 2015, http://www.osti.gov/scitech/servlets/purl/899269 (4/01/2016).

Highlights

- The efflorescence mineralogy showed a vertical distribution and changes over time.
- The mineral distribution is from interaction of RH diurnal changes and capillary flow.
- Over nine years the efflorescence developed after the intervention had reached the pre-intervention composition.
- Also simple salts, we found humberstonite, darapskite, konyaite and aphthitalite.
- Saline ions came mainly from groundwater and airborne particles.

elsevier_JCBM_7851

Queries and Answers

Query: Your article is registered as a regular item and is being processed for inclusion in a regular issue of the journal. If this is NOT correct and your article belongs to a Special Issue/Collection please contact c.samiullah@elsevier.com immediately prior to returning your corrections.
Answer: It not belong to a special collection.

Query: The author names have been tagged as given names and surnames (surnames are highlighted in teal color). Please confirm if they have been identified correctly.
Answer: The surname of La Igesia, the correct form, is **La Iglesia** Instituto de Geociencias (IGEO, CSIC, UCM), Facultad de Geología, c/ JoséAntonio Novais, 12, 28040 Madrid, Spain, this a mistake, the correct form is Instituto de Geociencias IGEO (CSIC, UCM), Facultad de Geología, c/ JoséAntonio Novais, 12, 28040 Madrid, Spain

Query: Please check the address for the corresponding author that has been added here, and correct if necessary.
Answer: It is ok.

Query: Please note that Fig. 3, Tables 5 and 7 were not cited in the text. Please check that the citations are in the appropriate place, and correct if necessary.
Answer: (Figs. 2A, 3A and 3B), are well located in the manuscript. Annual RH variation in Elche, calculated as the mean difference between extreme monthly average values ([RHmaximun (%) – RHmínimun (%)]/RHaverage) - – which are considerably higher than the daily average values - – shows coefficient of variation (CV) values below 6%.**Table 5 ...**The sodium (Eq. –%), related to Mg2+ = Na+/(Na+ + Mg2+), and nitrate (Eq. –%) related to SO42– = ΣN/(ΣN + S) was calculated from data obtained by Nicolas et al. [3], and provided an explanation for the presence of nitrates in the efflorescence. **Table 7**

Query: The opening quote does not have a corresponding closing quote in the sentence 'The MDRH is …'. Please insert the quote in the appropriate position.
Answer: "*The MDRH is always lower than the DRH of any single salt in the mixture*"

Query: A mismatch between the author name and corresponding reference number in the sentence "The humberstonite would be…". Please check and correct if necessary.
Answer: Vega et al. [**15]**

Query: As Refs. [57] and [61] were identical, the latter has been removed from the reference list and subsequent references have been renumbered.
Answer: OK. Thank you.